Ab initio simulation of structure in amorphous hydrogenated carbon

M. M. M. Bilek
Department of Engineering, University of Cambridge, Cambridge CB2 1PZ, United Kingdom

D. R. McKenzie
Department of Applied Physics, University of Sydney, Sydney, N.S.W. 2006, Australia

D. G. McCulloch
Department of Physics, RMIT University, Melbourne, Vic 3000, Australia

C. M. Goringe
Australian Key Centre for Microscopy and Microanalysis, University of Sydney, Sydney, N.S.W. 2006, Australia
(Received 28 June 1999; revised manuscript received 18 January 2000)

First-principles quantum molecular-dynamics simulations of the structure of hydrogenated amorphous carbon, *a*-C:H, at two densities (2.0 and 2.9 g/cm^3) have been carried out using the Car-Parrinello method. The results for the low-density structure show good agreement with experiment in the manner in which the hydrogen is incorporated, as judged by agreement with published vibrational density of states and neutron-diffraction data at various levels of deuteration. The simulation reproduces the position and magnitude of the hydrogen features in the pair-correlation function $G(r)$ obtained from neutron diffraction. The nonhydrogenated carbon atoms are predominantly sp^2 hybridized and the hydrogen atoms are largely ''sandwiched'' between layers of sp^2 atoms. The simulated high-density structure has a majority of nonhydrogenated carbon atoms with sp^3 hybridization. The results of this study show that a useful test for confirming the high-density *a*-C:H structure is the presence of a small C-C-C bond angle and the occurrence of C-H bond stretching frequencies above 3100 cm^{-1}.

I. INTRODUCTION

Hydrogenated amorphous carbon, also referred to as ''diamondlike carbon,'' is usually prepared by deposition from glow discharge plasmas containing hydrocarbon precursors. The material has properties which depend on the type of hydrocarbon precursor and on the deposition conditions, especially the temperature of the substrate and the incident energy of the depositing species. For a review of the subject of amorphous hydrogenated carbon films the reader is referred to the review of Robertson.[1]

The applications of the material make use of the properties of moderate hardness, low friction coefficient, and high chemical inertness. The material prepared in this way has a density of approximately 2 g/cm^3 and contains up to 30 at. % of hydrogen. ESR spectroscopy shows that annealing increases the number of unpaired electrons and as the heat treatment is extended to higher temperatures, the ESR signal from these electrons is reduced as the size of the graphitelike conjugated regions increases.[2] Annealing in a vacuum produces a change in the infrared-absorption spectrum which corresponds to the elimination of hydrogen initially held in CH_3 and CH_2 groups.[3] Structural studies[4–6] show the material consists largely of sp^2 hybridized carbon, with a small fraction of sp^3 carbon.

The preparation of a high-density form of hydrogenated carbon material has been reported.[7] This material has a density of 2.9 g/cm^3 and a hydrogen content of approximately 22–27 %.[8] A high degree of tetrahedral bonding of the carbon atoms is expected in this material which can be considered the hydrogenated equivalent of tetrahedral amorphous carbon (ta-C).

The aim of this work is to develop a structural model for *a*-C:H using *ab initio* molecular dynamics and compare it with observations. Previous simulations of *a*-C:H have used a nonorthogonal tight-binding method.[9,8] *Ab initio* models based on density-functional theory have successfully predicted structure in pure amorphous carbon materials[10–12] and so it is useful to apply them to the related hydrogenated materials, for which many experimental data exist.

In this study we produce detailed structural models for both a high-density and a low-density form of *a*-C:H for comparison with experimental diffraction data and to make predictions of physical properties which can be checked against experiment. Densities of 2.9 g/cm^3 and 2.0 g/cm^3 were chosen for the high- and low-density simulations, respectively. Although previous simulation work has been carried out on *a*-C:H,[8,13,9] these methods used a form of tight-binding technique whose results need to be checked against more accurate methods such as the density-functional methods. Tight-binding methods use a spherically symmetric repulsive potential which does not fully describe the strong anisotropy of the sp^2 hybridization. The tight-binding orbitals also give a less complete description of the electronic states than the large plane-wave basis set employed in the density-functional method used in this work.

II. THEORETICAL APPROACH

We have sought to apply the most accurate molecular-dynamics modeling techniques available which allow for the modeling of a sufficient number of atoms over a time scale long enough to reproduce the rapid quenching conditions applying to a film grown under energetic impacts. It has been

shown in previous work[11] that a cooling time of 500 fs is sufficient to represent the cooling of a thermal spike produced by an atom with 50 eV energy, incident on a carbon film. A first-principles molecular-dynamics scheme based on the calculation of forces from electronic wave functions calculated from density-functional theory in the generalized gradient approximation was therefore chosen as giving a good level of accuracy with a level of computational complexity amenable to a 64 atom system. A 64 atom system is large enough with periodic boundary conditions to give a reasonable simulation of an amorphous material with a single *k*-point sampling. We confirmed that for amorphous structures, a single *k* point for a 64 atom simulation gives good agreement with multiple *k* point simulation. The density-functional molecular-dynamics method of Car and Parrinello has been successfully applied to hydrogen-free amorphous carbon at a density of 2.0 g/cm^3 (Refs. 10 and 12) and a density of 2.9 g/cm^3,[11,12] guiding our choice of density for this study. In the Car-Parrinello technique, classical molecular dynamics of the atom cores is combined with fictitious dynamics for the electrons in which the expansion coefficients of the electron wave functions in a plane-wave expansion are the dynamical variables. The expansion coefficients of the electron waves are allowed to evolve in such a way as to maintain the system close to its minimum energy or *Born-Oppenheimer* surface at all times. The simulation is performed in three stages. First, a liquid is formed by the rapid melting of an unstable simple-cubic structure of the desired density. The system is allowed to mix during a constant temperature anneal at 5000 K for 360 fs, while the system is in contact with a thermostat of the Nose-Hoover type.[14,15]

Finally, the liquid is quenched to a solid by the removal of energy according to a predetermined exponential cooling curve over a period of 500 fs. In each case the plane-wave cutoff energy was 50 Ry. We simulate *a*-C:H at two different densities with a fixed composition of 12 hydrogen atoms and 52 carbon atoms. The atom cores were described by pseudopotentials of the Goedecker type.[16] Periodic boundary conditions were employed to eliminate surface effects, and a single *k* point at the center of the Brillouin zone of the periodically extended structure was used. Experimentally it is observed that in *a*-C:H there is a large variety of structure possible, and in some cases, a ''memory'' exists of the hydrocarbon precursor in plasma synthesis. In our liquid quench simulation, we attempt to remove all traces of the initial configuration by allowing the liquid to self-diffuse. Our simulation will therefore resemble those preparation methods which involve the most postdeposition modification of the precursors, which in plasma deposition are hydrocarbon fragments. These conditions are most likely to be achieved when the thermal spike is large and exists for a time similar to the duration of our simulation, approximately 500 fs. As noted above, this corresponds to approximately 50 eV impact energy. These conditions may be difficult to achieve experimentally, especially for the higher-density *a*-C:H material, since hydrogen may be readily eliminated from metastable configurations by the energetic impacts.

III. RESULTS AND DISCUSSION

Views of the two *a*-C:H networks are shown in Fig. 1. The two views of each structure were chosen to be orthogonal to one another. Figures 1(a) and 1(b) show the high-density structure. Figure 1(c) views the low-density structure along the planes, which correspond to the minimum stress directions of the diagonalized stress tensor. Figure 1(d) shows a view of the low-density structure looking along the direction perpendicular to the planes. In order to show the bonding environments of the boundary atoms we include in Fig. 1 the six adjacent unit cells implied by the periodic boundary conditions.

A. Stress tensor

The coordinate axes were rotated to diagonalize the stress tensors and thus align the axes with the principal stresses. This was done in order to determine the degree of anisotropy of the stress field. The stress tensors (values in GPa) in the thus rotated reference frames are

$$\begin{pmatrix} 46 & 0 & 0 \\ 0 & 22 & 0 \\ 0 & 0 & 14 \end{pmatrix}$$

and

$$\begin{pmatrix} -6 & 0 & 0 \\ 0 & 12 & 0 \\ 0 & 0 & 14 \end{pmatrix},$$

respectively. Table I compares the average stresses of our *a*-C:H structures with simulations of *a*-C (Ref. 12) and shows that the two structures at the same density have similar stress levels; in other words, the hydrogen is accommodated into the network without increasing the stress level.

B. Ring statistics

A useful way of comparing networks is to calculate the distribution of ring sizes using an appropriate definition of a ring. One such definition is the *shortest path ring* of Franzblau,[17] which is defined as a circuit for which there is no shortcut across the ring for any antipodal pair. The size distributions of carbon rings found in each of the structures are given in Table II where they are compared with data from a previously reported amorphous carbon calculation with density 2.9 g/cm^3.[12] The low-density structure has a preference for five, six, and seven membered rings, with seven being the most common number. This agrees with the results of Frauenheim[9] although there is a greater emphasis on seven membered rings in our work. The high-density structure shows a dominance of five membered rings compared to hydrogen free *a*-C at the same density. We also find that three membered rings have been eliminated entirely by hydrogenation.

C. Bond lengths and angles

Figures 2(a) and 2(b) show pair-correlation functions $G(r)$ calculated from each of the *a*-C:H structures. The position of the hydrogen peak is shifted to a lower distance (1.06 Å) in the high-density structure compared with the C-H distance of 1.1 Å found in the low-density structure. This

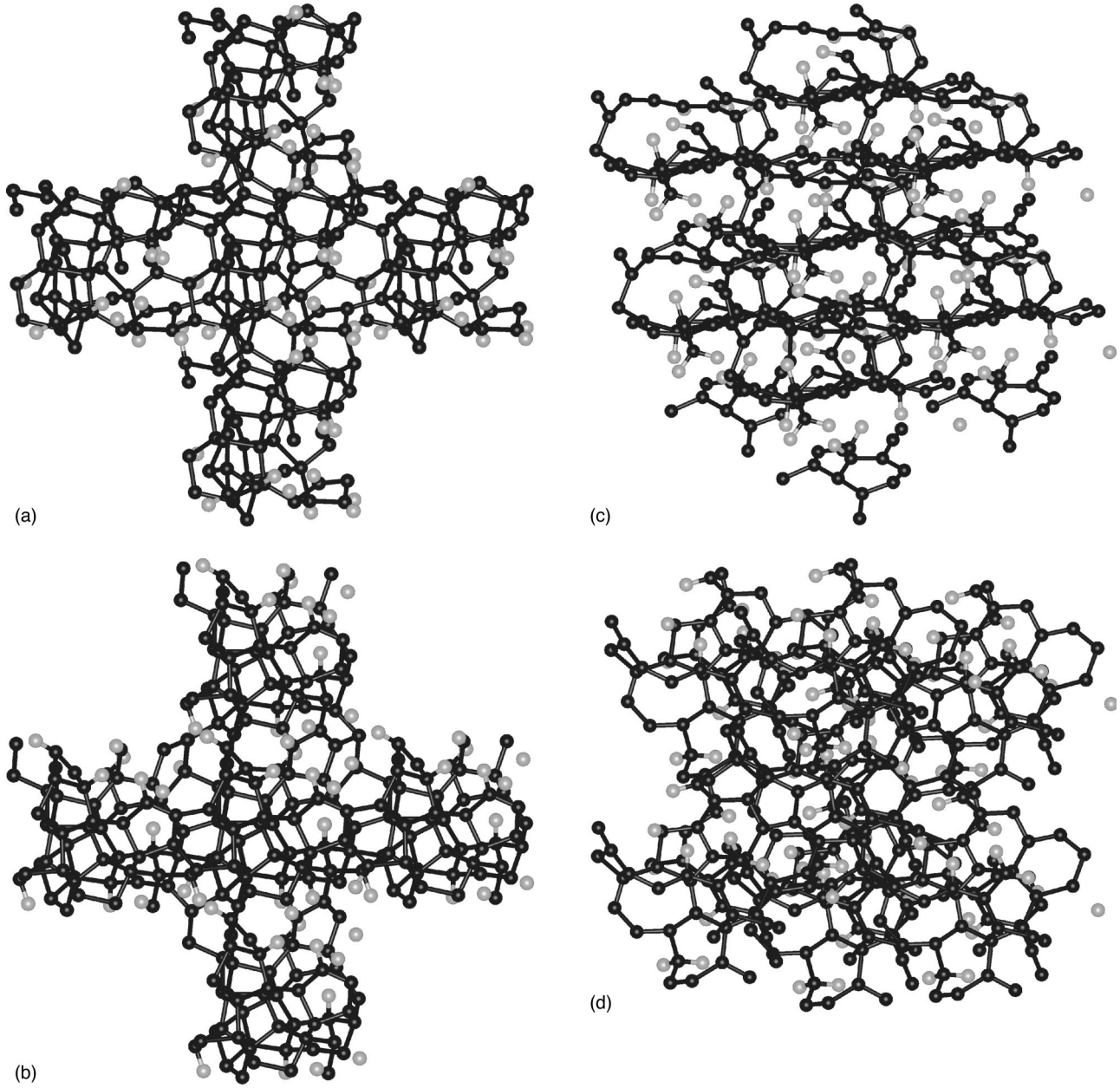

FIG. 1. (a) and (b) show views of the 2.9 g/cm^3 structure. The 2.0 g/cm^3 network is shown viewed (c) parallel to the graphitelike planes and (d) perpendicular to the planes (i.e. looking along the direction of lowest stress). The dark atoms correspond to carbon and the light ones to hydrogen.

shows that the hydrogen atoms are under considerable compression to allow them to be accommodated in the high-density structure.

Figures 2(b), 2(c), and 2(d) compare the $G(r)$ data calculated for our low-density (2.0 g/cm^3) network with the neutron-diffraction measurements of Burke *et al.*[5] The measurements were made on *a*-C:(H,D) material with three different compositions. In view of the opposite signs of the scattering lengths of H and D, these measurements clearly distinguish distances in the network which involve a hydrogen atom from those that do not and are therefore a more sensitive test of agreement between the simulation and observation than a single measurement on *a*-C:H. A distance

TABLE I. Average stress for *a*-C:H simulations compared with average stress for simulations of *a*-C of equivalent density, (Ref. 12).

Simulation	Average stress (GPa)	Optical gap (eV)
a-C:H (2.9 g/cm^3)	27.3	1.18 ± 0.2
a-C:H (2.0 g/cm^3)	6.7	-0.5 ± 0.5
a-C (2.9 g/cm^3)	28.0	-0.5 ± 0.2
a-C (2.0 g/cm^3)	6.0	-1.9 ± 0.2

TABLE II. Ring statistics.

Simulation	3	4	5	6	7	8	9
a-C:H (2.9 g/cm^3)	0	3	17	14	15	1	1
a-C:H (2.0 g/cm^3)	0	0	3	4	6	2	1
a-C (2.9 g/cm^3)	2	6	9	14	10	11	3

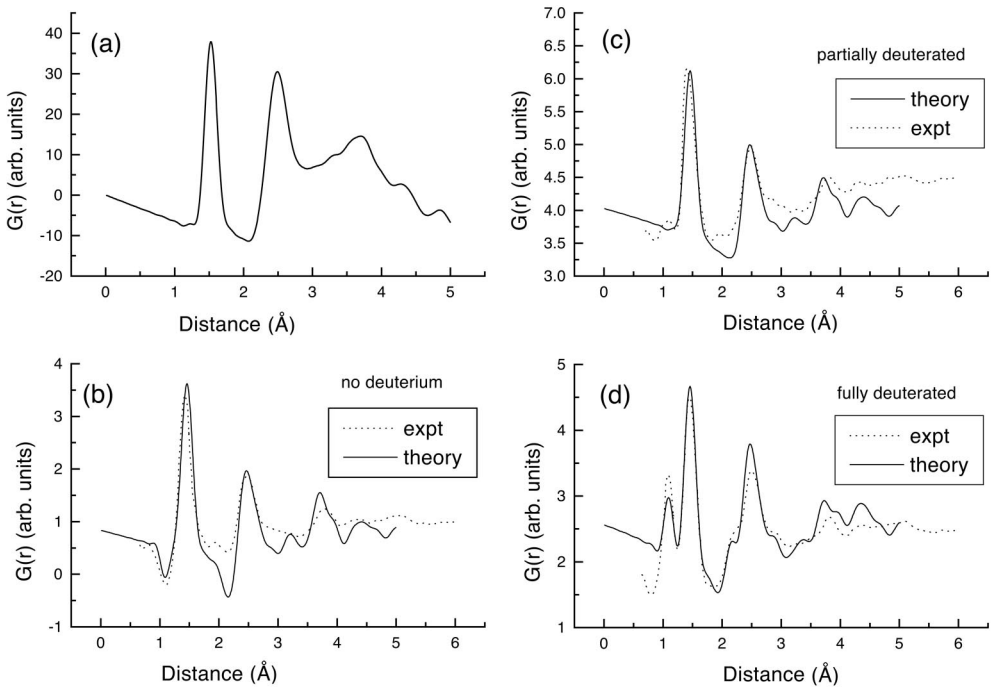

FIG. 2. Reduced density functions, $G(r)$, obtained from (a) the 2.9 g/cm^3 a-C:H structure and (b) the 2.0 g/cm^3 a-C:H structure. Neutron-diffraction data from a-$C_{0.75}$:$H_{0.25}$ (Ref. 5) are also shown for comparison. The plots given in (c) and (d) show comparisons between neutron-diffraction data published by Burke *et al.* (Ref. 5) for a-$C_{0.74}$:$D_{0.09}$:$H_{0.17}$ and a-$C_{0.73}$:$D_{0.27}$, respectively, with theoretical calculations obtained from our 2.0 g/cm^3 structure using scattering factors which account for the presence of the deuterium.

which includes at least one hydrogen atom changes from a negative feature to a positive feature in the $G(r)$. Examples of such distances are indicated in the figure at 1.1, 2.15 and 2.87 Å. The species involved in each of the distances can be determined by detailed examination of the network. The distance of 1.1 Å arises from C-H bonds. The 2.15 Å separation has contributions from both C-H and H-H pairs. There are 23 distances in the range 2.15 ± 0.055 Å all of which involve hydrogen. Of these 13% are H-H pairs and the rest are C-H pairs. In the range of 2.87 ± 0.05 Å there are 16 C-C, 16 C-H and 2 H-H distances. A shoulder appears at this position in both the simulated and experimental curves for the the fully deuterated case. It is not as pronounced as the previously mentioned features because of the smaller fraction of hydrogen containing distances. There is good agreement between simulation and experiment in both the position and magnitude of the features involving hydrogen, indicating that the simulation is able to reproduce the characteristics of the hydrogen incorporation.

Nearest-neighbor distances and bond angles obtained from the $G(r)$ curves together with statistics describing the distribution of carbon coordinations observed and the number of CH_2 and CH groups found in each structure are given in Table III. The results show that the sp^3 fraction increases with the addition of hydrogen at both densities. This trend is also evident in the work of Frauenheim *et al.*,[9] although we observe a more dramatic effect, with the fraction going from 6% to 16% as compared with 19% to 23%. The fact that the calculated values of sp^3 fraction are higher in the work of Frauenheim *et al.* may be partly attributed to their calculation being at a somewhat higher density of 2.2 g/cm^3.

D. Topology of the networks

The high-density (2.9 g/cm^3) structure is dominated by tetrahedrally bonded carbon. Even among carbon atoms which are not bonded to hydrogen there is a majority of sp^3 hybridized atoms. The sp^2 carbon atoms have a tendency to occur in chains. There are $12sp^2$ atoms forming one chain of four, one chain of three, and a chain of two. The remaining three are not bonded to other sp^2 atoms, but in all cases hydrogen is closely associated. Two of the others are bonded

TABLE III. Nearest-neighbor distances and percentage coordination calculated for carbon atoms in various networks.

	Neighbors		Coordination No. %								
Simulation	1st	2nd	1	2	3	4	5	Ave. Coord.	Bond angle (°)	No. CH_2	No. CH
a-C:H (2.9 g/cm^3)	1.52	2.44	0	0.27	23.42	75.18	1.13	3.77	106.8	0	12
a-C:H (2.0 g/cm^3)	1.46	2.46	0	10.96	73.08	15.96	0	3.05	114.8	2	8
a-C (2.9 g/cm^3)	1.50	2.51	0	0	50	50	0	3.5	114	NA	NA
a-C (2.0 g/cm^3)	1.47	2.53	0	15.2	78.4	6.4	0	2.9	118.8	NA	NA

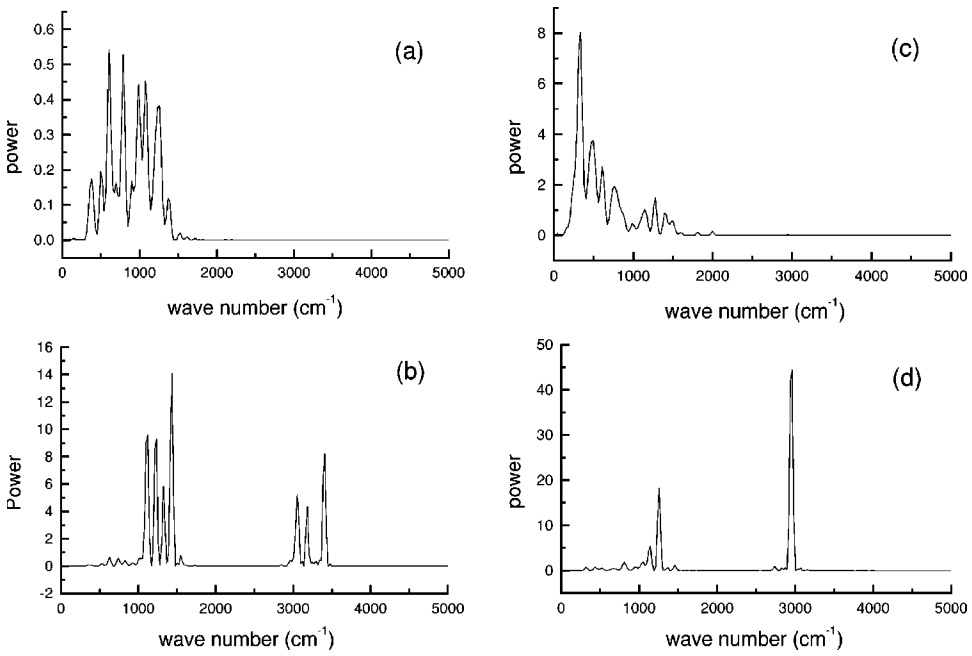

FIG. 3. Vibrational density-of-states spectra calculated from (a) the carbon and (b) the hydrogen atoms in the 2.9 g/cm^3 structure, and from (c) the carbon and (d) the hydrogen atoms of the 2.0 g/cm^3 structure.

to sp^3 atoms which have a C-H bond and the other has a C-H bond itself. The hydrogen atoms in the high-density network are all monohydrides and there are some quite close H-H approaches.

The low-density structure is dominated by sp^2 carbon and shows a strong tendency to form graphitelike planes as shown in Fig. 1(c) where the structure has been rotated so that the *c*-axis-like direction is vertical. The tendency to form planes can be quantified by summing the bond lengths projected onto the axis normal to the planes and comparing this with the sum of bond lengths projected onto the two in-plane directions. The graphitelike anisotropy of the structure is demonstrated by the fact that the total bond length projected onto the *c*-axis-like direction amounts to 95.9 Å which is significantly lower than that calculated for two orthogonal directions (123.5 and 125.3). The planes are somewhat buckled and cross-linked in a number of places by sp^3 bonds between atoms of adjacent sheets. The hydrogen atoms tend to be attached to the surfaces of the sheets in C-H ''monohydride'' or C-H_2 ''dihydride'' configurations, so that a hydrogen rich layer is sandwiched between the carbon layers. There are examples of monohydride hydrogen atoms attached to aromatic (sp^2 bonded) ring structures as well as to sp^3 bonded atoms, although there is a preference for hydrogen atoms to be bonded to an sp^3 hybridized carbon atom. Of the 12 hydrogen atoms in the structure, 7 are bonded to sp^3 carbon atoms even though there are only 8 sp^3 atoms in the low-density structure in total. This shows that the nonhydrogenated part of the low-density network is mostly sp^2 bonded. These sp^3 atoms tend to be included in sp^2 bonded rings with the bond to the hydrogen atom directed perpendicular to the plane of the ring.

E. Vibrational DOS

Vibrational density of states (VDOS) spectra calculated from velocity-velocity autocorrelation functions of the carbon and hydrogen atoms separately are shown in Fig. 3. The VDOS for hydrogen atoms shows strong maxima in the region of C-H stretching modes in the vicinity of 3000 cm^{-1} and in the region of bending modes below 1600 cm^{-1}. As expected, the VDOS for carbon atoms does not show features in the C-H stretching region, because the large mass difference between C and H ensures that the carbon atom motion in such vibrations is very small. The carbon VDOS shows additional features below 2000 cm^{-1} which are consistent with the vibrations of the C-C network. The low-density VDOS agree with experimental infrared absorption for *a*-C:H films of similar density in that the C-H stretching spectrum is confined to a relatively narrow region around 3000 cm^{-1}.

For the high-density material, this is no longer the case and the C-H stretching modes become spread over a wider region above 3000 cm^{-1}. This is a key prediction of our simulations and can be regarded as a signature of a high-density ta-C:H film which could be tested experimentally.

In order to identify which atoms in the structure produced the C-H vibrations above 3000 cm^{-1}, we calculated an individual VDOS for each hydrogen atom. We found that two hydrogens bonded to opposite sides of a four membered ring were producing the C-H stretching mode of the highest frequency at $\sim$3400 cm^{-1}. These are the only hydrogen atoms bonded to a four membered ring, all the others are on five or six membered rings. These hydrogens have nonbonded carbon atoms at distances of 1.77 Å and 1.85 Å, the closest nonbonded C-H distances in the structure. Such close interactions would have the effect of increasing the oscillation frequency.

F. Electronic DOS

The electronic density of states (EDOS) of the networks was calculated from the Kohn-Sham eigenvalues. Jones and Gunnarsson[18] have discussed the fact that while these eigen-

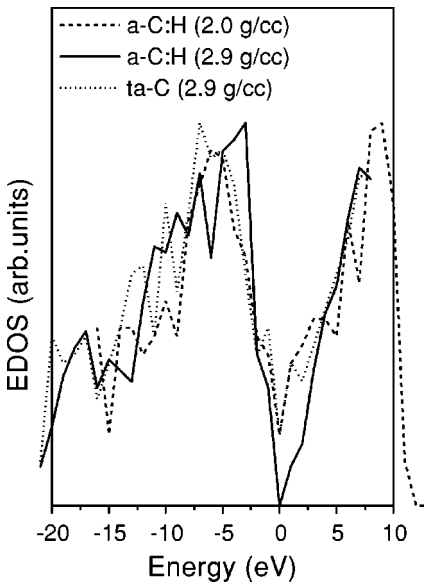

FIG. 4. The electronic density of states for 2.0 g/cm^3 and 2.9 g/cm^3 a-C:H structures and a 2.9 g/cm^3 a-C structure.

values have not yet been shown to have a relation with the real eigenvalues of the electronic Hamiltonian, they agree well with excitation energies at least in the case of semiconductors. We compare in Fig. 4 the EDOS as calculated from the distribution of Kohn-Sham eigenvalues for the two a-C:H networks with a ta-C network of density of 2.9 g/cm^3.

The results show that hydrogenation of the network at a density of 2.0 g/cm^3 gives a band gap similar to a pure carbon network with a density of 2.9 g/cm^3. This agrees with the fact that both a-C:H and ta-C are observed to be rather transparent in the visible spectrum. Hydrogenation at a density of 2.9 g/cm^3 produces a pronounced deepening of the minimum in the gap DOS compared with a pure carbon network of the same density. This is in agreement with the observed effect of bonded hydrogen of eliminating some states in the gap region resulting in a strong increase in transparency and a reduction in electrical conductivity.

G. Optical properties

The optical or Tauc gap (E_{opt}) in an amorphous semiconductor is defined by

$$\hbar\omega\sqrt{\epsilon_2} = B(\hbar\omega - E_{\text{opt}}), \tag{1}$$

where B is a constant. The dielectric permittivity ϵ_2 can be calculated from the convolution integral

$$\epsilon_2 = \frac{1}{\omega^2}\int g_0(E)g_u(E+\hbar\omega)dE, \tag{2}$$

where g_o is the DOS for occupied states below the Fermi energy and g_u is the DOS for unoccupied states above the Fermi energy. The value of E_{opt} is obtained from the linear part of the plot and is shown in Table I. The uncertainty ranges are determined from the range of possible fits to the approximate straight section of the plot.

The gaps have small or even negative values. This underestimation is expected because of the finite cell size and the generalized gradient approximation which, like the local-density approximation, underestimates the band gap in semiconductors. The values of the optical gap are therefore to be used only for comparative purposes. Hydrogenation clearly increases the band gap, as does an increase in sp^3 fraction.

IV. CONCLUSIONS

The calculations show that the characteristics of the simulated low-density a-C:H structure compare well with experiment in many structural details. The manner in which hydrogen is incorporated is well reproduced as indicated by the good agreement with neutron diffraction at three levels of deuteration. Other points of agreement are the presence of a layered structure in the carbon framework; the existence of large C-C bond angles approaching 120°; the coordination number of approximately three; and the vibrational density of states showing C-H stretching in the vicinity of 3000 cm^{-1}.

Our simulations indicate that a high-density hydrogenated carbon structure with a majority of the nonhydrogenated carbon atoms in a tetrahedral configuration could be created experimentally under favorable conditions. However, there is insufficient experimental data so far to achieve the level of comparison between theory and experiment that we have been able to achieve with the low-density structure. Nevertheless, our simulation results provide tests for the existence of this high-density form of a-C:H. These are the presence of a small C-C-C bond angle, even smaller than the tetrahedral value, a shortened C-H bond length, and the presence of some exceptionally high C-H infrared bond-stretching frequencies above 3100 cm^{-1}. When compared with the nonhydrogenated forms of carbon at the same density the hydrogenated form has a larger electronic and optical gap.

ACKNOWLEDGMENTS

The authors wish to thank M. Parrinello for permission to use the CPMD program and Dr. J. Hutter for helpful advice concerning its operation. This work was supported by Emmanuel College, Cambridge, for which M. Bilek would like to thank the college.

[1] J. Robertson, Adv. Phys. **35**, 317 (1986).
[2] D. J. Miller and D. R. McKenzie, Thin Solid Films **108**, 257 (1983).
[3] D. R. McKenzie, R. C. McPhedran, N. Savvides, and L. C. Botten, Philos. Mag. B **48**, 341 (1983).
[4] J. K. Walters, P. J. R. Honeybone, D. W. Huxley, R. J. Newport, and W. S. Howells, Phys. Rev. B **50**, 831 (1994).
[5] T. M. Burke, R. J. Newport, W. S. Howells, K. W. R. Gilkes, and P. H. Gaskell, J. Non-Cryst. Solids **166**, 1139 (1993).
[6] J. K. Walters, C. D. Algar, T. M. Burke, J. S. Rigden, R. J.

Newport, G. Bushnellwye, W. S. Howells, S. Sattel, M. Weiler, and H. J. Ehrhardt, J. Non-Cryst. Solids **197**, 41 (1996).
[7] M. Weiler, S. Sattel, K. Jung, H. J. Ehrhardt, and V. S. Veerasamy, Diamond Relat. Mater. **3**, 608 (1994).
[8] T. Frauenheim, G. Jungnickel, U. Stephan, P. Blaudeck, S. Deutschmann, M. Weiler, S. Sattel, K. Jung, and H. Ehrhardt, Phys. Rev. B **50**, 7940 (1994).
[9] T. Frauenheim, P. Blaudeck, U. Stephan, and G. Jungnickel, Phys. Rev. B **48**, 4823 (1993).
[10] G. Galli, R. Martin, R. Car, and M. Parrinello, Phys. Rev. B **42**, 7470 (1990).
[11] N. A. Marks, D. R. McKenzie, B. A. Pailthorpe, M. Bernasconi, and M. Parrinello, Phys. Rev. B **54**, 9703 (1996).
[12] D. G. McCulloch, D. R. McKenzie, and C. M. Goringe, Phys. Rev. B **61**, 2349 (2000).
[13] G. Jungnickel, T. Frauenheim, D. Porezag, P. Blaudeck, and U. Stephan, Phys. Rev. B **50**, 6709 (1994).
[14] S. Nose, Mol. Phys. **52**, 255 (1984).
[15] W. Hoover, Phys. Rev. A **31**, 1695 (1985).
[16] S. Goedecker, M. Teter, and J. Hutter, Phys. Rev. B **54**, 1703 (1996).
[17] D. S. Franzblau, Phys. Rev. B **44**, 4925 (1991).
[18] R. Jones and O. Gunnarsson, Rev. Mod. Phys. **61**, 689 (1989).